

Antiferromagnetic order in weakly coupled random spin chains

J. Kokalj¹, J. Herbrych², A. Zheludev³, and P. Prelovšek^{1,4}

¹*J. Stefan Institute, SI-1000 Ljubljana, Slovenia*

²*Crete Center for Quantum Complexity and Nanotechnology, Department of Physics, University of Crete, P.O. Box 2208, 71003 Heraklion, Greece*

³*Neutron Scattering and Magnetism, Laboratory for Solid State Physics, ETH Zürich, Zürich, Switzerland and*

⁴*Faculty of Mathematics and Physics, University of Ljubljana, SI-1000 Ljubljana, Slovenia*

(Dated: March 2, 2022)

The ordering of weakly coupled random antiferromagnetic $S = 1/2$ chains, as relevant for recent experimentally investigated spin chain materials, is considered theoretically. The one-dimensional isotropic Heisenberg model with random exchange interactions is treated numerically on finite chains with the density-matrix renormalization-group approach as well as with the standard renormalization analysis, both within the mean-field approximation for interchain coupling J_{\perp} . Results for the ordering temperature T_N and for the ordered moment m_0 are presented and are both reduced with the increasing disorder agreeing with experimental observations. The most pronounced effect of the random singlet concept appears to be a very large span of local ordered moments, becoming wider with decreasing J_{\perp} , consistent with μ SR experimental findings.

PACS numbers: 05.60.Gg, 25.40.Fq, 71.27.+a, 75.10.Pq

I. INTRODUCTION

The antiferromagnetic (AFM) Heisenberg model of $S = 1/2$ spins on a one-dimensional (1D) chain represents one of the prototype and most studied quantum many-body model for strongly correlated electrons, being at the same time realized nearly perfectly in several materials. Since 1D spin systems do not exhibit any long range order even at temperature $T = 0$, the ordering appears through the interchain coupling. The ordering Néel temperature T_N emerging in weakly coupled AFM chains is by now well described theoretically¹, being confirmed by numerical calculations² and experimental investigations on materials with quasi-1D spin systems³.

The quenched disorder in intrachain exchange couplings reveals in 1D spin chains qualitatively new phenomena as well theoretical and experimental challenges. Even in the case of unfrustrated AFM random Heisenberg chain (RHC) it has been shown using the renormalization-group (RG) approaches⁴⁻⁷ that the $T \rightarrow 0$ behavior is qualitatively changed by any disorder leading to the concept of random singlets (RS). The signature of such state is the singular - Curie-like - divergence of the uniform susceptibility $\chi_0(T \rightarrow 0)$ ⁸. Such behavior was also found for exactly solvable model of impurities coupled with random exchange interactions to the host Heisenberg chain, but only for strong randomness⁹. Refreshed theoretical interest in RHC phenomena has been stimulated by the synthesis and experimental investigations of novel materials representing the realization of RHC, in particular $\text{BaCu}_2(\text{Si}_{1-x}\text{Ge}_x)_2\text{O}_7$ ^{3,10,11} and $\text{Cu}(\text{py})_2(\text{Cl}_{1-x}\text{Br}_x)_2$ ¹² compounds. Experiments confirmed theoretically predicted $\chi_0(T)$ ¹³, but revealed also novel features as large and strongly T -dependent spread of local NMR spin-lattice relaxation times^{11,14} which has been reproduced within the simple RHC model¹⁵.

The existence of weak but finite interchain couplings J_{\perp} in quasi-1D RHC compounds and related AFM ordering at low $T < T_N$ open a new perspective on the RS systems¹². Mixed $\text{BaCu}_2(\text{Si}_{1-x}\text{Ge}_x)_2\text{O}_7$ ¹⁰ as well $\text{Cu}(\text{py})_2(\text{Cl}_{1-x}\text{Br}_x)_2$ ¹² show

a substantial reduction of T_N as well as the ground state (g.s.) $T = 0$ ordered magnetic moment m_0 relative to the disorder-free ($x = 0, 1$) materials. Theoretical treatments so far suggested even the opposite trend¹⁶ revealing the difficulties of theoretical approaches. The central theoretical issue also in connection with experiments is to what extent and in which properties the singular behavior of quantum RS physics remains reflected in the long-range AFM order at low T . The aim of this paper is to present results of numerical and analytical calculations which show that under the presence of weak (but not extremely weak) interchain coupling treated within a mean-field approximation (MFA) randomness reduces both T_N as well as m_0 , which is in agreement with experiment. We also present evidence that the RS phenomena is reflected in large distribution of $T = 0$ local ordered moments m_i being consistent with preliminary experimental results¹⁷.

The paper is organised as follows. In Section II we introduce the model and the MFA approximation. In Section III we introduce the numerical method and present results on staggered susceptibility and transition temperature. This is followed by presentation of results for ordered moments and their distribution in Section IV. In Section V we discuss results obtained by RG and in Section VI we compare our results in more detail with experiment. Conclusions are given at the end in Section VII.

II. MODEL

Our goal is to understand properties in particular the ordering in the quasi-1D RHC model, which is given by quenched (intrachain) random exchange couplings $J_{i,j}$ and constant interchain coupling J_{\perp} ,

$$H = \sum_{i,j} J_{i,j} \mathbf{S}_{i,j} \cdot \mathbf{S}_{i+1,j} + J_{\perp} \sum_{i,\langle jj' \rangle} \mathbf{S}_{i,j} \cdot \mathbf{S}_{i,j'}, \quad (1)$$

where \mathbf{S} are $S = 1/2$ spin operators. The isotropic Heisenberg coupling is assumed both within the chain ($J_{i,j}$ with i

denoting sites in the chain and j denoting different chains) as well as for the interchain term and $\langle jj' \rangle$ run over z_\perp nearest-neighbor chains. E.g., neutron scattering results for pure system¹⁸ BaCu₂Si₂O₇ show that the interlayer coupling is in fact only twice weaker than the intralayer one. Taking into account also a further non-frustrating diagonal coupling J_3 the MFA becomes rather well justified at least on the lowest non-trivial level. Further more, in the same reference¹⁸ it has been shown, that for the pure non-random chain using the MFA with the proper $z_\perp = 4$ and $J_\perp = (1/4)[2|J_x| + 2|J_y| + 4|J_3|] \ll J_z$ yields very good estimates for T_N and m_0 . Here we used the same notation as in Ref. 18 with J_z being intra-chain coupling, J_x and J_y interchain couplings and J_3 inter-chain non-frustrating diagonal coupling. We therefore adopt the same z_\perp and use for comparison to experiments the same J_\perp . This holds also for doped material, but with less clear role of disorder on J_\perp which we discuss again in Section VI.

Still we expect in analogy to other quasi-1D spin systems^{1,2} that the main ordering features should be captured by the MFA for interchain coupling and by the effective 1D RHC with the staggered field h_s provided that $J_\perp \ll J_i$,

$$H^{\text{MF}} = \sum_i J_i \mathbf{S}_i \cdot \mathbf{S}_{i+1} - h_s \sum_i (-1)^i S_i^z. \quad (2)$$

Within the MFA the staggered field is given by $h_s = -z_\perp J_\perp m_s$ with the staggered magnetization $m_s = (1/L) \sum_i (-1)^i \langle S_i^z \rangle$ and $\langle \dots \rangle$ denoting thermal average. We will further on consider random quenched J_i and assume their distribution to be uncorrelated uniform boxed distribution with $J - \delta J \leq J_i \leq J + \delta J$ and $\delta J < J$. For experimental examples more appropriate distribution would be binary one, but it has been verified¹⁵ that qualitative features do not depend essentially on the form of the distribution. In the following we use units $J = 1$ and set $k_B = \hbar = 1$.

III. STAGGERED SUSCEPTIBILITY AND NÉEL TEMPERATURE

Within the MFA for the interchain coupling the instability towards the AFM ordering and the ordering temperature T_N are determined by the staggered static susceptibility χ_π of a 1D chain and the relation^{1,16,19,20}

$$z_\perp |J_\perp| \chi_\pi(T_N) = 1. \quad (3)$$

Such a relation is commonly derived within the random phase approximation approach but is generally coming from the selfconsistency (linear response) relation at the transition $m_s = \chi_\pi(T_N) h_s$ independent whether the system is clean^{1,19} or disordered within the chain^{16,20}. Clearly, it is valid within MFA since h_s is assumed as the averaged one, while $\chi_\pi(T)$ corresponds to a macroscopic value (equivalent to disorder averaged one). It is expected that even in strongly disordered systems the conditions for Eq. (3) are well satisfied for $z_\perp |J_\perp| \ll J$. It should however be noted that some quantitative correction as discussed for clean systems^{2,21,22} ($z_\perp \rightarrow k z_\perp$ with $k < 1$ due to quantum fluctuations) to Eq. (3) might be relevant.

We evaluate $m_s(T)$ and $\chi_\pi(T)$ using the finite-temperature dynamical density matrix renormalization group (FTD-DMRG) method^{23,24} on a finite chain with L sites and open boundary conditions. In the FTD-DMRG method standard $T = 0$ DMRG targeting of ground state density matrix $\rho^0 = |0\rangle\langle 0|$ is generalized with finite- T density matrix $\rho^T = (1/Z) \sum_n |n\rangle e^{-H/T} \langle n|$. Next, the reduced density matrix is calculated and then truncated in the standard DMRG-like manner for basis optimization. The limitation of the FTD-DMRG method are at low T finite-size effects, which are rather small due to large accessible system with DMRG algorithm and which are even further reduced with randomness.

The quenched random J_i are introduced into the DMRG procedure at the beginning of *finite* algorithm. *Infinite* algorithm is preformed for homogeneous system $J_i = J$ and the randomness of J_i is introduced in the first sweep. In this way the preparation of the basis in the *infinite* algorithm is performed just once and for all realizations of J_i -s, while larger number of sweeps (usually ~ 5) is needed to converge the basis within the *finite* algorithm for random J_i . After *finite* algorithm, magnetization $\langle S_i^z \rangle$ at desired T is calculated at every site of the chain within *measurements* part of DMRG procedure. Furthermore, for systems with $\delta J > 0$ we employ also random configuration averaging and typically $N_r = 10$ realizations for finite- T is sufficient due to χ_π being macroscopic quantity with modest fluctuations between different disorder realizations. For $T = 0$ we use smaller $N_r = 5$, since standard DMRG method and larger systems ($L = 800$) can be used.

χ_π can be evaluated via dynamical susceptibility $\chi''(\pi, \omega)$, still we use mostly the alternative approach by evaluating m_s at finite T and h_s , and then using $\chi_\pi(T) = \lim_{h_s \rightarrow 0} m_s(T, h_s)/h_s$. Within this approach numerical results are more robust or reliable since only static quantities are calculated and finite size or boundary effects can be reduced, e.g., by considering only sites close to the middle of a chain. Still, limit $h_s \rightarrow 0$ is hard to reach numerically, but at finite T small field $h_s \sim 0.01$ suffices.

Results for χ_π used to extract T_N with Eq. (3) are for several δJ shown in Fig. 1a. For $\delta J = 0$ analytical approaches²⁵⁻²⁷ suggest that for $T \rightarrow 0$

$$\chi_\pi^p = a \sqrt{\ln(b/T)}/T, \quad (4)$$

and also higher order corrections are discussed²⁸. Results for random $\delta J \neq 0$ shown in Fig. 1a clearly indicate that increasing δJ reduces χ_π and consequently leads to a systematic decrease of T_N (for fixed J_\perp and J) as shown in Fig. 1b. Fig. 1a also reveals that $\chi_\pi(T)$ qualitatively changes with increasing disorder. While for pure case the $T \rightarrow 0$ behavior in Eq. (4) is well followed, for large $\delta J > 0.5$ we find that

$$\chi_\pi^{RS} = c [T \ln^2(d/T)]^{-1}, \quad (5)$$

established by RS and with a modified RG approach discussed further on, fits numerical results better. Since our temperature span is quite limited ($0.1 < T < 0.25$ for $\delta J = 0$ and $0.05 < T < 0.25$ for $\delta J = 0.8$) we can not extract precise values of the parameters and even less comment on the

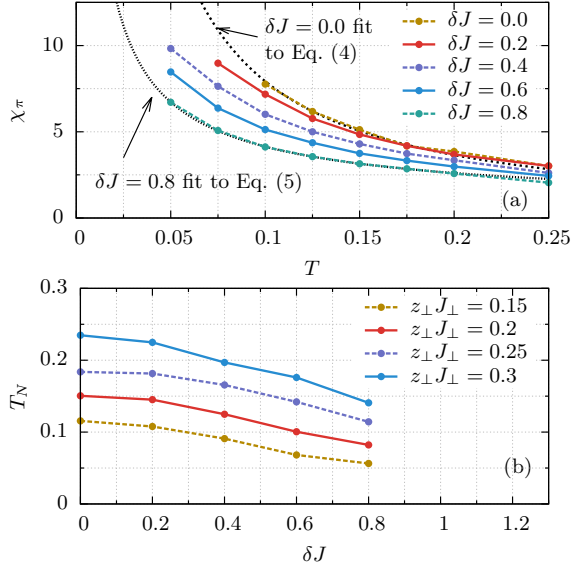


Figure 1. (Color online) (a) T dependence of χ_π for various randomness δJ . Black, dashed line represents RS fit, Eq. (5), for $\delta J = 0.8$. Shown is also a fit for pure case to Eq. (4). (b) Decrease of Néel temperature T_N with randomness δJ for various $z_\perp J_\perp$. Calculated with $L = 80$.

functional forms. However, numerically obtained staggered susceptibility $\chi_\pi(T)$ for random system ($\delta J = 0.8$) is better fitted or described with Eq. (5) than Eq. (4) and vice versa for the pure case ($\delta J = 0$). Note that in the latter case, quantum Monte Carlo gives^{29,30} $a \simeq 0.30$ – 0.32 and $b \simeq 5.9$ – 9.8 , while for random case this is the first report (see Appendix A) (at least to our knowledge) of the estimated parameter values.

Experimentally significant $T_N/J \lesssim 0.02$ ($J_\perp/J \lesssim 0.02$)^{10,18} requires $\chi_\pi \gtrsim 12.5$ (with $z_\perp = 4$), which is at present beyond the reach of the FTD-DMRG method. In order to analyse T_N we chose modest values of $z_\perp J_\perp = 0.15, \dots, 0.3$, presented in Fig. 1b. Still, for the smallest considered $z_\perp J_\perp = 0.15$ we get reduction of T_N by a factor of ~ 2 for $\delta J = 0.8$. This is in contrast to previous RG study¹⁶ discussed later on, but in agreement with experimental observations^{10,12,17}.

IV. STAGGERED ORDERED MOMENT

In order to determine the $T = 0$ average staggered ordered moment m_0 for particular J_\perp and disorder δJ as a solution to MFA self-consistency relation $-h_s/(z_\perp J_\perp) = m_s(h_s)$, we first evaluate the g.s. $m_s(h_s)$. Again finite-size effects are largest for the pure case ($\delta J = 0$) but in reliable regime ($h_s > 0.0001$) we can make a comparison to the analytical result obtained from Ref. 1,

$$m_s^p = r(h_s)^g, \quad (6)$$

with $r = 0.637$ and $g = 1/3$. In Fig. 2b we compare Eq. (6) to our DMRG results and reveal substantial differences. Our

$m_s(h_s)$ for $\delta J = 0$ shows rather stronger increase with h_s , which cannot be reconciled with Eq. (6) simply by just increasing prefactor r . Linear dependence shown in Fig. 2b suggests different exponent ($g \neq 1/3$) or possibly some logarithmic corrections.

Results in Fig. 2a,b show that disorder δJ leads to a decrease of staggered magnetization m_s in our h_s -regime. A possibility of increased m_s with increased δJ remains at very low $h_s < 0.0001$ as suggested in Fig. 2b. We investigate and discuss it later also with the use of RG method. Ordered moment m_0 and its decrease with δJ for different values of $z_\perp J_\perp$ is presented in Fig. 2c.

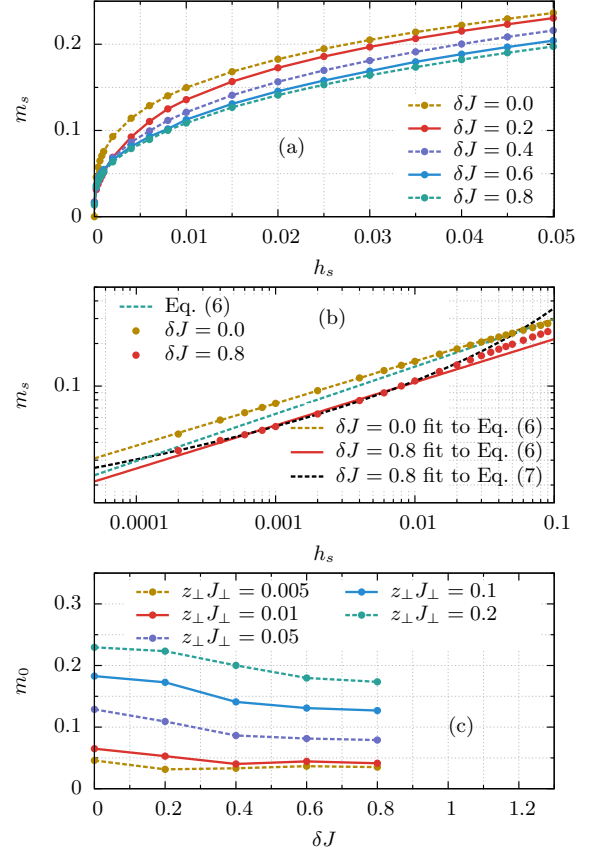


Figure 2. (Color online) (a) $T = 0$ staggered magnetization m_s vs. h_s for various randomness δJ . (b) Log-log plot of m_s vs. h_s for $\delta J = 0, 0.8$. $m_s(h_s)$ for $\delta J = 0$ deviates from prediction in Eq. (6) in exponent g and prefactor r . The result for $\delta J = 0.8$ shows a RS like behavior given with Eq. (7). Fits of parameters for Eq. (6) or (7) are for regime $0.0001 < h < 0.01$. (c) Self-consistent solution for staggered magnetization m_0 vs. δJ for different $z_\perp J_\perp$.

A novel feature introduced by disorder is the distribution of local ordered moments. To avoid the influence of open boundary conditions we calculate local staggered $m_i = (-1)^i \langle S_i^z \rangle$ from the middle of the chain modeled with Eq. (2) and for the MFA self-consistent fields h_s at particular $z_\perp J_\perp$. Even in a uniform staggered field h_s moments m_i are found to vary from site to site and depend on the concrete random configuration J_i . We present the probability distribution func-

tion (PDF) in Fig. 3a for different randomness δJ and fixed $z_{\perp}J_{\perp} = 0.05$, while in Fig. 3b we show it for fixed δJ and different $z_{\perp}J_{\perp}$. It is evident from Fig. 3a that for large disorder and small $z_{\perp}J_{\perp}$ the PDF largely deviate from the Gaussian-like form. Moreover, the relative spread of distribution $\Delta = \sigma_{m_i}/m_0$ can become even $\Delta > 1$.

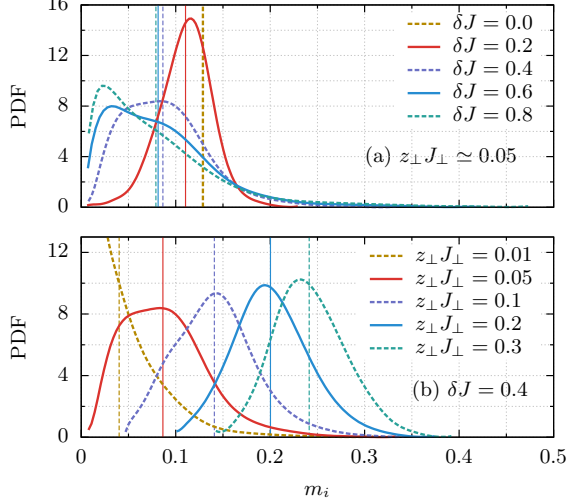


Figure 3. (Color online) Probability distribution function of m_i at $T = 0$ for (a) various values of δJ and fixed $z_{\perp}J_{\perp} = 0.05$, and (b) for fixed $\delta J = 0.4$ and various $z_{\perp}J_{\perp}$. Thin, vertical lines represent m_0 for given δJ and J_{\perp} .

V. REAL SPACE RENORMALIZATION GROUP

For better understanding and interpretation of above results within the RS concept we perform similar real space renormalization group procedure as introduced by Dasgupta and Ma⁵ and used also in Ref. 16 and where strongest bonds are eliminated and reduced effective coupling J_{eff} is introduced. We generalized the procedure for finite h_s and calculation of m_s and give more technical details in the Appendix B. We perform RG procedure numerically on a large system and by carrying it to the end together with evaluation of staggered magnetization for different starting staggered fields we obtain $m_s(h_s)$ for $T = 0$. A simple RS argument suggest that in a finite h_s all spins with effective coupling $J_{\text{eff}} < h_s$ are fully polarized, while the ones with $J_{\text{eff}} > h_s$ form singlets and contribute only weakly to the staggered magnetization. Since the portion of spins with $J_{\text{eff}} < h_s$ in a RS theory is $\propto \ln^{-2}(n/h_s)$ ⁵, one expects for small h_s

$$m_s^{RS}(h_s) \propto \ln^{-2}(n/h_s). \quad (7)$$

We confirm this RS prediction with our numerical RG (Appendix B), and $T = 0$ DMRG results shown in Fig. 2b at low h_s , since they deviate from simple power law behavior of Eq. (6) (linear in log-log plot) with a substantial upward curvature, nicely captured with Eq. (7). Our result in Fig. 2b

therefore represents one of a few^{14,31,32} confirmations of the RS phenomenology.

With RG procedure one can make also predictions for finite- T results (see Refs. 5 and 6), which are obtained by performing RG steps as long as some Hamiltonian parameter (e.g. exchange coupling) is larger than T , while for the remaining system with all effective parameters below T , a high T result is used. In our case with the system in finite magnetic field h_s , these fields do not get reduced with RG and therefore roughly set the lowest energy scale. This means that for $T < h_s$ one can perform the RG to the end and obtain $T = 0$ result for all $T < h_s$. Once T becomes above h_s all steps with $J < h_s$ cannot be performed and for this remaining system the high- T result (m_s roughly linear in h_s) should be used. This leads for $h_s \ll T$ to a random singlet like prediction for staggered magnetization $m_s = h_s c [T \ln^2(d/T)]^{-1}$, and straightforwardly for the staggered susceptibility given in Eq. (5). Staggered susceptibility has the same functional form as a RS prediction for uniform susceptibility^{6,8,13} $\chi_0(T)$, which can be expected for random system with no translational symmetry and strongly local correlations. In Fig. 1a we show that our numerical calculations with FTD-DMRG give support to this RS prediction.

VI. COMPARISON WITH EXPERIMENT

Turning to the experimental realizations of random spin chains, two systems have been studied so far with magnetic ordering at low T , namely $\text{BaCu}_2(\text{Si}_{1-x}\text{Ge}_x)_2\text{O}_7$ ^{10,11,17} and $\text{Cu}(\text{py})_2(\text{Cl}_{1-x}\text{Br}_x)_2$ ¹², and for the former a clear evidence of 1D RS physics has already been detected for $T > T_N$ ^{11,15}. Its magnetic properties can be well described by a simple bimodal distribution of AFM in-chain exchange constants¹¹, namely $J_i = J_1, J_2$ with probabilities x and $1 - x$, respectively, and by weak interchain coupling $J_{\perp} \ll J_i$. Although our treatment assumes a uniform distribution of the exchange constants, it should be able to capture general features of $\text{BaCu}_2(\text{Si}_{1-x}\text{Ge}_x)_2\text{O}_7$, particularly with Ge concentration $x \sim 0.5$ ¹⁵.

The experimental data that are most relevant to our calculations are μ -SR experiments, from which the magnitude of m_0 can be inferred. In full agreement with our predictions, in both $\text{Cu}(\text{py})_2(\text{Cl}_{1-x}\text{Br}_x)_2$ ¹² and $\text{BaCu}_2(\text{Si}_{1-x}\text{Ge}_x)_2\text{O}_7$ ¹⁷, m_0 and the ordering temperature T_N were found to *decrease* with increasing disorder. This said, the drop in $\text{BaCu}_2(\text{Si}_{1-x}\text{Ge}_x)_2\text{O}_7$ appears more abrupt than predicted. One of the possibility would be that the strength of J_{\perp} and even its sign may be locally affected by disorder as observed in Ref. 10. This may also be an indication of MFA limitations and possibility that a wide distribution with long tails of local moments or effective local fields used in the MFA (not taken into account due to used constant averaged field h_s), could affect the results. It is thus compelling to check, if initial staggered field h_s in Eq. (2) should be taken from adequate distribution of the local moments $\{h_i\} = -z_{\perp}J_{\perp}\{m_i\}$ and if wide distribution of initial h_i fields could affect the results in Fig. 3. We check this in two ways: (i) by taking ran-

dom h_i with exponential distribution, and (ii) by taking the distribution of m_i (and thus h_i) from another realization of J_i . Fig. 4 depicts comparison between these two methods, together with constant staggered field (as in Fig. 3) calculated for $L = 800$ and one fixed realization of J_i . In Fig. 4a we present three distributions of the staggered magnetic fields h_s and in Fig. 4b corresponding cumulative distribution function (CDF) of magnetic moment m_i . It is clear from the later that the distribution of m_i do not depend strongly on distribution of h_i and even more importantly for MFA, all considered distributions give very similar averages of m_i . We would like to note that in Fig. 4 we present one of the most critical cases with small averaged fields with resulting very broad distribution of m_i , and that even in this case the constant fields or fields with very wide distribution give very similar results for distribution of moments.

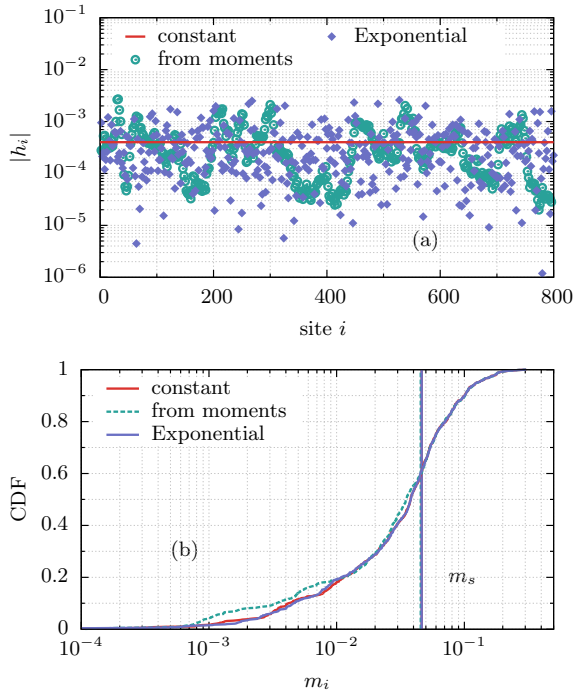


Figure 4. (Color online) Dependence of the magnetic moment distribution (for fixed J_i) on the magnetic field used in the mean-field approximation, as calculated for $L = 800$ sites. Panel (a) shows three distributions of staggered fields with the same average value $\langle |h_i| \rangle = 0.0004$; constant one, exponential distribution, and distribution from numerical simulations (see text for details). Panel (b) shows corresponding cumulative distribution function (CDF) of magnetic moment m_i . Vertical lines represent values of average m_s , which are practically the same for all three distributions of h_i .

The most interesting experimental observation for $\text{BaCu}_2(\text{Si}_{1-x}\text{Ge}_x)_2\text{O}_7$ is a drastic broadening of the distribution of local static moments in the magnetically ordered state¹⁷. This behavior is consistent with our predictions borne in Fig. 3. Unfortunately, making a quantitative comparison beyond a qualitative agreement is not feasible at present, since μ -SR measures the distribution of local magnetic fields, not magnetic moments. Due to the presence of several

crystallographic muon sites, the m_0 distribution can not be unambiguously extracted from such experiments.

VII. CONCLUSIONS

In conclusion, we have shown that at fixed average J and interchain coupling J_\perp the disorder $\delta J > 0$ leads to a decrease of Néel temperature T_N as well as to reduced g.s. ordered staggered moment m_0 , in a very broad range of $\delta J > 0$ (and regime studied here). This is due to χ_π being smaller for random system than for a pure system in a relevant regime (see Fig. 1a), which is in contrast with the uniform susceptibility $\chi_0(T \rightarrow 0)$ which approaches constant for pure case but diverges $\propto 1/[T \ln^2(\tilde{\beta}/T)]$ for $\delta J > 0$. This is analogous to Eq. (5) and a direct signature of RS scenario leading at low T to formation of local singlets and almost free spins. The effect of disorder at $q = \pi$ is less dramatic than for $q = 0$ since to the leading order (neglecting log corrections) both pure and $\delta J > 0$ cases reveal $\chi_\pi \propto 1/T$. However, in a random case χ_π is still larger than χ_0 (same holds also for structure factor as shown in Fig. 15 in Ref. 31) and the system still tends to AFM order.

Numerical results for $m_s(h_s)$ at $T = 0$ in Fig. 2a,b show that in the regime with larger h_s (e.g., $h_s > 0.0001$ for $\delta J = 0.8$) the average moment m_s (and in turn m_0 shown in Fig. 2c) decreases with increasing δJ . On the other hand, Eqs. (6), (7) and results in Fig. 2 suggest a regime of very low h_s where m_s (m_0) could be increased by $\delta J > 0$. This could be relevant only for larger δJ and for very small J_\perp ($\lesssim 0.001$ for $\delta J = 0.8$) which would lead to enhanced T_N and m_0 with increased δJ or in other words, to *order by disorder*. Such behavior was actually predicted by MFA and RG treatment¹⁶, but is contrary to the one mainly discussed here, as well not found in materials of interest¹⁷.

The most striking effect of the RHC physics and of anomalous RS response in the ordered phase is however the distribution of local moments m_i , as manifested by $\text{PDF}(m_i)$ in Fig. 3. It is evident that the relative distribution width Δ increases with δJ but even more importantly with decreasing $z_\perp J_\perp$. This is a clear indication that anomalous width originates in the RS physics and is not trivially related to initial δJ . For example, the same or constant δJ results in increased relative width of distribution (Δ), if $z_\perp J_\perp$ is decreased (see Fig. 3b). It should be noted that for larger δJ even $m_i < 0$ becomes possible (moments m_i locally opposite to local fields)¹⁴. This means that at small $J_\perp \ll J$ and strongly reduced T_N the PDF width can become large, i.e. $\Delta \sim 1$.

Regarding the experiment, our results of decreasing m_0 and ordering temperature T_N with increasing disorder agree with observations of the μ -SR experiments on $\text{Cu}(\text{py})_2(\text{Cl}_{1-x}\text{Br}_x)_2$ ¹² and $\text{BaCu}_2(\text{Si}_{1-x}\text{Ge}_x)_2\text{O}_7$ ¹⁷. Furthermore, we are able to capture with the microscopic model the interesting experimental observation of the drastic broadening of the distribution of local static moments in the magnetically ordered state of $\text{BaCu}_2(\text{Si}_{1-x}\text{Ge}_x)_2\text{O}_7$ ¹⁷.

ACKNOWLEDGMENTS

We acknowledge helpful and inspiring discussions with M. Thede. We acknowledge the support of the European Union program (J.H.) FP7-REGPOT-2012-2013-1 no. 316165 and of the Slovenian Research Agency under program (P.P.) P1-0044 and under grant (J.K.) Z1-5442.

Appendix A: Temperature fits

	Eq. (4)		Eq. (5)	
	a	b	c	d
$\delta J = 0$	0.3702	9.8	1898	$\rightarrow \infty$
$\delta J = 0.8$	0.0647	$\rightarrow \infty$	18.55	82.56

Table I. Values of fitted parameters of Eq. (4) and Eq. (5) to the pure ($\delta J = 0$) and random ($\delta J = 0.8$) datasets (see Fig. 1).

Appendix B: RG procedure

We numerically performed similar renormalization group procedure as introduced by Dasgupta and Ma⁵ and modified it to include the staggered magnetic field h_s and extended it for calculation of staggered magnetization m_s , similarly as done in Ref. 16. In the original procedure the bonds with largest J_i were eliminated which we replace by subsequent elimination of bonds with largest J_i^{xx} . In the presence of broken rotational symmetry due to staggered magnetic field h_s , J_i^{xx} does not equal J_i^{zz} at further steps of the elimination process. In the case of $h_s = 0$ the criteria equals to the original one used by Dasgupta and Ma⁵ and $J_i^{xx} = J_i^{zz}$. Justification of J_i^{xx} for elimination criteria is also that it is the only non-diagonal element of the Hamiltonian and that for $J_i^{xx} = 0$ the ground state is a simple product state or Neél state, which can be exactly obtained by arbitrary order of the elimination steps provided that elimination is performed to the end. For finite- T properties also other energy scales like J_i^{zz} and h_i are important and need to be considered.

Once the bond of two sites to eliminate are chosen we integrate them out by the following procedure. First we calculate eigenstates of the four site Hamiltonian which consists of two sites to be eliminated (namely sites 2 and 3) plus two neighboring sites (namely sites 1 and 4). Usually the relevant states which we would like to keep are the four lowest states and from which we could build effective Hamiltonian or the new bond (from site 1 to 4) parameters. However, as the elimination procedure advances the four lowest states of the four site Hamiltonian do not necessarily have the character of the ground state on eliminated bond (sites 2, 3) i.e. they do not all have large overlap with it and some state with the character of higher lying state on sites 2 and 3 might become low and among first four low lying states of the four site Hamiltonian. This does not happen if $J_{12}^{xx,zz}$ and $J_{34}^{xx,zz}$ are much smaller than $J_{23}^{xx,zz}$. In such case we choose four eigenstates of the 4 site Hamiltonian with the largest overlap with the ground state on eliminated two sites (sites 2, 3). These four states span the part of the relevant low energy Hilbert space that we would like to keep and are close to the states kept in the second order procedure in Ref. 5.

From this four states ($|\psi_i\rangle$ with energy E_i , $i = 1, \dots, 4$) we build new effective Hamiltonian for the remaining sites (sites 1, 4) by first constructing $H_{1234} = \sum_i |\psi_i\rangle E_i \langle\psi_i|$ and then tracing out the eliminated sites $H_{14} = \sum_{i_{23}} \langle i_{23} | H_{1234} | i_{23} \rangle$. Here $|i_{23}\rangle$ are basis states for eliminated sites (sites 2, 3). New H_{14} is the new Hamiltonian in the basis of remaining sites (1 and 4) and from which one can read new effective parameters like J_{14}^{xx} , J_{14}^{zz} , h_1 , h_4 and energy of integrated out sites E_{23} .

Similar procedure can be used for determining the parameters of new operators that we are interested in. For example, operator $a_1 S_1^z + a_2 S_2^z + a_3 S_3^z + a_4 S_4^z$ is transformed into new operator $\tilde{a}_1 S_1^z + \tilde{a}_4 S_4^z + o_{23}$ after integrating out sites (2 and 3), while in this case the parameters \tilde{a}_1 , \tilde{a}_4 and o_{23} need to be optimally chosen and small relative error (typically of 10^{-6}) can appear by approximating the operator in the basis for remaining sites (1 and 4) by just three parameters.

In this way one eliminates the two sites, obtains new effective parameters for the Hamiltonian and operator on the new bond (connecting site 1 and 4) and can proceed with the new step of RG or by choosing next two sites to eliminate. The ground state energy and expectation value of the operator in the ground state are obtained by performing the RG to the end (eliminate all sites) and summing all E_{23} and o_{23} for the energy and the operator expectation values, respectively.

¹ H. J. Schulz, *Phys. Rev. Lett.* **77**, 2790 (1996).

² C. Yasuda, S. Todo, K. Hukushima, F. Alet, M. Keller, M. Troyer, and H. Takayama, *Phys. Rev. Lett.* **94**, 217201 (2005).

³ I. Tsukada, Y. Sasago, K. Uchinokura, A. Zheludev, S. Maslov, G. Shirane, K. Kakurai, and E. Ressouche, *Phys. Rev. B* **60**, 6601 (1999).

⁴ S.-k. Ma, C. Dasgupta, and C.-k. Hu, *Phys. Rev. Lett.* **43**, 1434 (1979).

⁵ C. Dasgupta and S.-k. Ma, *Phys. Rev. B* **22**, 1305 (1980).

⁶ D. S. Fisher, *Phys. Rev. B* **50**, 3799 (1994).

⁷ E. Westerberg, A. Furusaki, M. Sigrist, and P. A. Lee, *Phys. Rev. Lett.* **75**, 4302 (1995).

⁸ J. E. Hirsch, *Phys. Rev. B* **22**, 5355 (1980).

⁹ A. Klümper and A. A. Zvyagin, *Phys. Rev. Lett.* **81**, 4975 (1998).

¹⁰ T. Yamada, Z. Hiroi, and M. Takano, *J. Solid State Chem.* **156**, 101 (2001).

¹¹ T. Shiroka, F. Casola, V. Glazkov, A. Zheludev, K. Prša, H.-R. Ott, and J. Mesot, *Phys. Rev. Lett.* **106**, 137202 (2011).

¹² M. Thede, F. Xiao, C. Baines, C. Landee, E. Morenzoni, and A. Zheludev, *Phys. Rev. B* **86**, 180407 (2012).

- ¹³ A. Zheludev, T. Masuda, G. Dhalenne, A. Revcolevschi, C. Frost, and T. Perring, *Phys. Rev. B* **75**, 054409 (2007).
- ¹⁴ T. Shiroka, F. Casola, W. Lorenz, K. Prša, A. Zheludev, H.-R. Ott, and J. Mesot, *Phys. Rev. B* **88**, 054422 (2013).
- ¹⁵ J. Herbrych, J. Kokalj, and P. Prelovšek, *Phys. Rev. Lett.* **111**, 147203 (2013).
- ¹⁶ A. Joshi and K. Yang, *Phys. Rev. B* **67**, 174403 (2003).
- ¹⁷ M. Thede, T. Haku, T. Masuda, C. Baines, E. Pomjakushina, G. Dhalenne, A. Revcolevschi, E. Morenzoni, and A. Zheludev, *Phys. Rev. B* **90**, 144407 (2014).
- ¹⁸ M. Kenzelmann, A. Zheludev, S. Raymond, E. Ressouche, T. Masuda, P. Böni, K. Kakurai, I. Tsukada, K. Uchinokura, and R. Coldea, *Phys. Rev. B* **64**, 054422 (2001).
- ¹⁹ D. J. Scalapino, Y. Imry, and P. Pincus, *Phys. Rev. B* **11**, 2042 (1975).
- ²⁰ E. Yusuf and K. Yang, *Phys. Rev. B* **72**, 020403 (2005).
- ²¹ V. Y. Irkhin and A. A. Katanin, *Phys. Rev. B* **61**, 6757 (2000).
- ²² M. Bocquet, *Phys. Rev. B* **65**, 184415 (2002).
- ²³ J. Kokalj and P. Prelovšek, *Phys. Rev. B* **80**, 205117 (2009).
- ²⁴ For details of numerical method see Supplemental Material of Ref. 15.
- ²⁵ T. Giamarchi and H. J. Schulz, *Phys. Rev. B* **39**, 4620 (1989).
- ²⁶ R. R. P. Singh, M. E. Fisher, and R. Shankar, *Phys. Rev. B* **39**, 2562 (1989).
- ²⁷ I. Affleck, D. Gepner, T. Ziman, and H. J. Schulz, *J. Phys. A: Math. Gen.* **22**, 511 (1989).
- ²⁸ V. Barzykin, *Phys. Rev. B* **63**, 140412 (2001).
- ²⁹ O. A. Starykh, A. W. Sandvik, and R. R. P. Singh, *Phys. Rev. B* **55**, 14953 (1997).
- ³⁰ Y. Kim, M. Greven, U.-J. Wiese, and R. Birgeneau, *Eur. Phys. J. B* **4**, 291 (1998).
- ³¹ J. A. Hoyos, A. P. Vieira, N. Laflorencie, and E. Miranda, *Phys. Rev. B* **76**, 174425 (2007).
- ³² K. Hida, *J. Phys. Soc. Jpn.* **65**, 895 (1996).